

Multi Sensor Data Fusion Using a Generalized Feature Model Applied to Different Types of Extended Road Objects

Heiko Cramer, Ullrich Scheunert, Gerd Wanielik
Chemnitz University of Technology
Reichenhainer Str. 70
09126 Chemnitz, Germany
{cramer, scheunert, wanielik}@infotech.tu-chemnitz.de

Abstract – The paper describes the usage of the generalized feature model in a multi sensor tracking system. The generalized feature model is based on the assumption that an object can be modelled by an individual set of features. This approach takes into account that objects have an actual size and can be measured by several different sensors. In this article different types of 3D road objects are considered and feature models for these types of object are introduced. The focus is mainly on the detection and tracking of pedestrians and vehicles in road environments. The particular problem of feature uncertainties in the generalized feature model is discussed using several sensor types. Also, different suitable dynamic models are applied to the feature model. The results are presented on the basis of simulations and real measurements.

Keywords: feature model, 3D model, Kalman filter, multi sensor multi target tracking

1 Introduction

Driver assistance systems become more and more relevant in the research field of information fusion because the usage of several sensors and different information to capture the environment around a car is important for these applications. This complex dynamic system consists of the sensor carrying vehicle and the traffic situation around it. The traffic situation can mainly be divided into two categories: the road in front of the vehicle, represented by the road parameters, and the objects on and beside the road. For tracking the objects (mainly pedestrians and vehicles) in the surroundings of the sensor carrying car, the estimation theory is suitable and often used (e.g. [1]-[2]). Here, a set of Kalman filters work in parallel and measurements are given from different sensors. In comparison to Kalman filter tracking in the field of air traffic control, one main difference for automotive applications is that objects can not be seen as point targets. The actual size of objects becomes important and has to be taken into account. Therefore, a generalized three-dimensional model for the multi sensor case was developed in our department [3]. This generalized feature model is based on the assumption that any entity in the world can be detected and recognized by means of features. It combines the approach of using 3D models with single sensors (e.g. [4]-[5]) with the approaches for tracking objects with more than one sensor ([6], [7]). The idea of using features can also be found in [8]. Features are assumed to be dedicated parts of the entity with certain spatio-temporal coordinates

in the coordinate system of the entity. However, features do not exist without being associated with a certain sensory principle and system. Therefore, in [3] every feature is

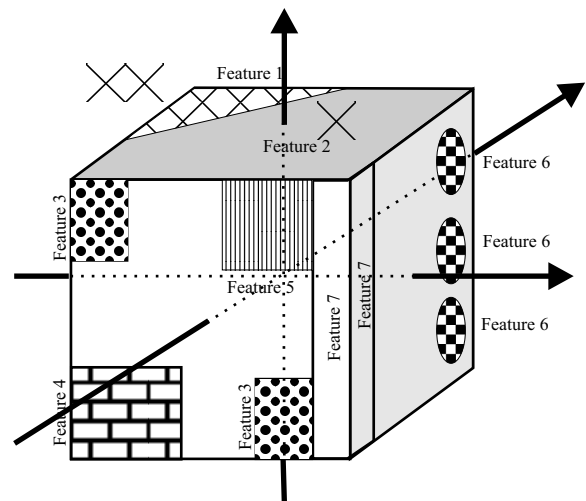


Fig. 1: General 3D feature model

linked to one or more specific sensor. To visualize this approach, figure 1 shows an abstract entity as a set of several features. It shows a cube that is attached to the features, while the features occur in designated 3-D positions.

While [3] describes the basics of the generalized feature model, in this paper we present the usage of different sensors, different object models and simulation results on the generalized feature model. The next section describes the uncertainty of features and how this influences the state estimation of a Kalman filter. In section 3, the focus is on different dynamic models to track obstacles in the surroundings and on the movement compensation of the sensor carrying car. While different dynamic models are used for different obstacle classes, the feature descriptions are also different not only for different sensors, but also for different objects. This is explained in section 4. A special approach for the usage of the generalized feature model together with a laser scanner is described in more detail in section 5. Using different models for several object types, the question arises, how it can be known, which object type is entering

the sensor's field of view when new detections occur. The first basic approaches are discussed in section 6. The conclusion and results can be found in the last section.

2 Uncertainty Description of Features

One main advantage of the Kalman filter theory is that for every estimated value also the uncertainty is also calculated. This is modelled by random numbers with the assumption that they are gaussian distributed ([9], [10]). The state space description of a system includes the process noise $\mathbf{v}(t_k)$

$$\mathbf{x}(t_{k+1}) = A(t_k)\mathbf{x}(t_k) + \mathbf{v}(t_k) \quad (1)$$

and the measurements are added by the measurement noise $\mathbf{w}(t_k)$

$$\mathbf{y}(t_k) = C(t_k)\mathbf{x}(t_k) + \mathbf{w}(t_k). \quad (2)$$

If the generalized feature model is used, this noise description has to be adapted and completed. This is done in the following part of this section. For every defined feature an individual uncertainty can be defined. Moreover, the feature is located in a specific position on an object (for example, a vehicle). This point is also not absolutely known and this uncertainty can be described by an additional random number. This leads to the assumption that four uncertainties have to be taken into account while using the feature model:

- The uncertainty of the state (objects position)
- The uncertainty of the feature's position on the object
- The uncertainty of the feature itself
- the uncertainty of the sensor system

To illustrate these uncertainty descriptions an example is introduced. For simplification, the time index t_k is ignored in this example. Figure 2 shows a tracked object (a vehicle), which is attached with a single point feature. This

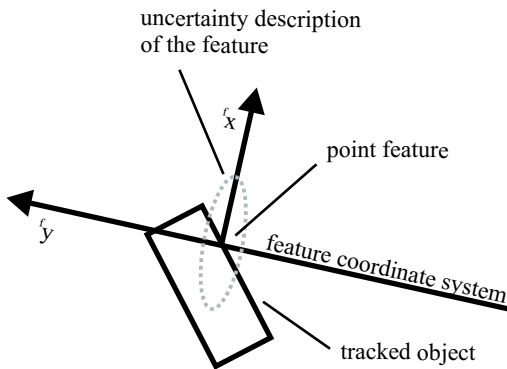


Fig. 2: Feature uncertainty

is located in the two dimensional coordinate system of the feature. The uncertainty is modelled by a random number with gaussian distribution and the mean value is equal to zero. The feature can therefore be written as

$${}^f\mathbf{x}_f = {}^f\mathbf{x}_{f0} + {}^f\mathbf{v}_f, \quad (3)$$

where the upper left index f denotes that the description is done in the space of the feature, namely the feature coordinate system. ${}^f\mathbf{x}_{f0}$ is the undisturbed position of the feature in the feature coordinate system and ${}^f\mathbf{v}_f$ describes the noise of this position. Often, ${}^f\mathbf{x}_{f0}$ is set to zero, if the feature is located in the origin of the feature coordinate system.

The transformation of the feature into the object coordinate system (figure 3) can be written as

$${}^o\mathbf{x}_f = g_{f \rightarrow o}({}^o\mathbf{x}_{f0}, {}^f\mathbf{x}_f) + {}^o\mathbf{v}_f. \quad (4)$$

In this equation, ${}^o\mathbf{x}_f$ is the description of the feature in the object coordinate system (denoted by the upper left index o) and ${}^o\mathbf{v}_f$ is a random value describing the uncertainty of the position of the feature. Including the definition that ${}^f\mathbf{x}_{f0}$ is zero, and equation (3) the feature in the object coordinate system is given with

$${}^o\mathbf{x}_f = g_{f \rightarrow o}({}^o\mathbf{x}_{f0}, {}^f\mathbf{v}_f) + {}^o\mathbf{v}_f. \quad (5)$$

In the case, that $g_{f \rightarrow o}$ describes the rotation and displace-

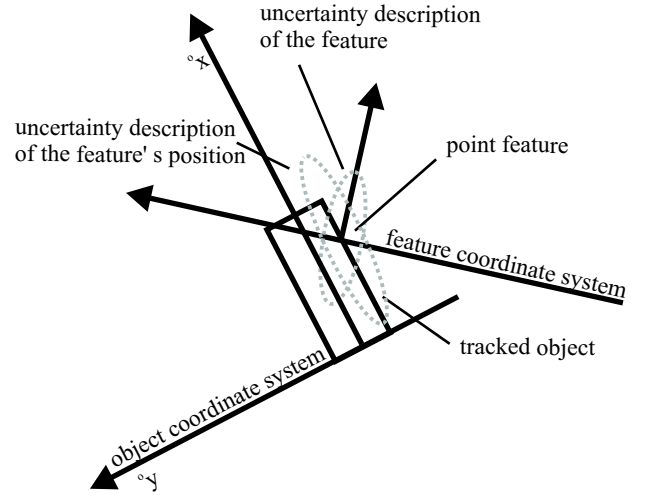


Fig. 3: Feature uncertainty in object coordinate system

ment of the feature coordinate system according to the object coordinate system, a linear expression of (5) could be given with

$${}^o\mathbf{x}_f = {}^o\mathbf{x}_{f0} + {}^o\mathbf{v}_f + C_{f \rightarrow o} {}^f\mathbf{v}_f, \quad (6)$$

where $C_{f \rightarrow o}$ describes the rotation and ${}^o\mathbf{x}_{f0}$ the undisturbed translation. This linear case of rotation and translation is just an example to illustrate the description of the uncertainty of the feature model. In the following sections, the rotation angles are not always independent from the state space and these transformations are therefore not linear.

The next transformation of a feature is from the object coordinate system to the sensor carrying vehicle coordinate system:

$${}^v\mathbf{x}_f = g_{o \rightarrow v}({}^v\mathbf{x}_{o0}, {}^o\mathbf{x}_f) + {}^v\mathbf{v}_o. \quad (7)$$

Here, ${}^v\mathbf{v}_o$ denotes the random error of the object's position in the vehicle coordinate system and ${}^v\mathbf{x}_f$ is the feature description in the vehicle coordinate system. In the example

being used, this transformation could also be written as a linear function (see figure 4).

$${}^v\mathbf{x}_f = {}^v\mathbf{x}_{o0} + {}^v\mathbf{v}_o + C_{o \rightarrow v} {}^o\mathbf{x}_f \quad (8)$$

Combining (6) and (8) leads to the full linear description of a feature in the vehicle coordinate system including all uncertainties:

$${}^v\mathbf{x}_f = {}^v\mathbf{x}_{o0} + {}^v\mathbf{v}_o + C_{o \rightarrow v} ({}^o\mathbf{x}_{f0} + {}^o\mathbf{v}_f + C_{f \rightarrow o} {}^f\mathbf{v}_f). \quad (9)$$

The complete nonlinear transformation is given with (5) and (7) and leads to

$${}^v\mathbf{x}_f = g_{o \rightarrow v}({}^v\mathbf{x}_{o0}, (g_{f \rightarrow o}({}^o\mathbf{x}_{f0}, {}^f\mathbf{v}_f) + {}^o\mathbf{v}_f)) + {}^v\mathbf{v}_o. \quad (10)$$

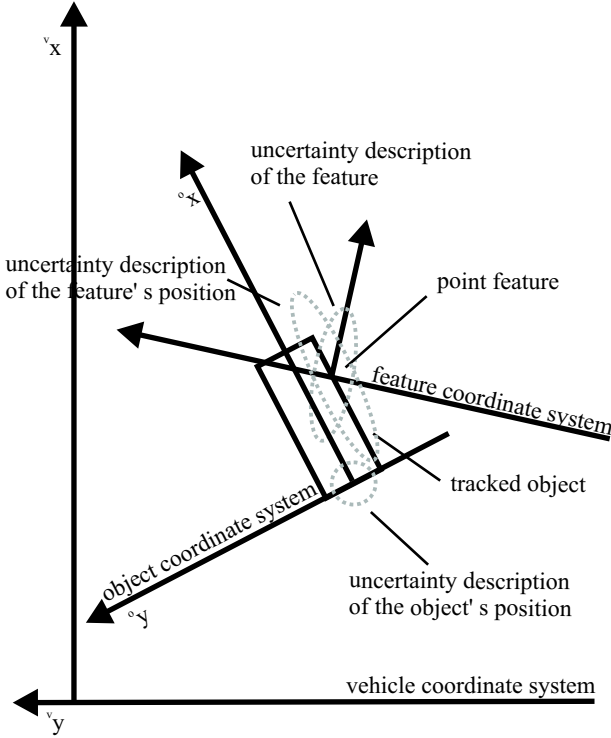


Fig. 4: Feature uncertainty in vehicle coordinate system

The random error variables are unknown in the usage of the described feature model in an Kalman filter. Therefore, the calculation of the expectation values of the vectors and the covariance is necessary

$${}^v\hat{\mathbf{x}}_f = E\{{}^v\mathbf{x}_f\}, \quad (11)$$

$${}^vP_f = E\{{}^v\mathbf{x}_f {}^v\mathbf{x}_f^T\}, \quad (12)$$

where $\hat{\mathbf{x}}$ denotes the estimated vector of \mathbf{x} , and P is the covariance of \mathbf{x} . The derivations are presented for the linear case first.

The mean value ${}^v\hat{\mathbf{x}}_f$ can be calculated by using (9) and the definition for random variables given with

$$E\{{}^v\mathbf{v}_o\} = 0, \quad E\{{}^o\mathbf{v}_f\} = 0 \quad \text{and} \quad E\{{}^f\mathbf{v}_f\} = 0. \quad (13)$$

The vectors without distribution are equal to their expectation values and this leads to the estimated mean value

$${}^v\hat{\mathbf{x}}_f = E\{{}^v\mathbf{x}_{o0} + C_{o \rightarrow v} {}^o\mathbf{x}_{f0}\} = {}^v\mathbf{x}_{o0} + C_{o \rightarrow v} {}^o\mathbf{x}_{f0}. \quad (14)$$

Calculating the uncertainty description, the variances of the undisturbed values are zero

$$E\{{}^v\mathbf{x}_{o0} {}^v\mathbf{x}_{o0}^T\} = 0, \quad E\{{}^o\mathbf{x}_{f0} {}^o\mathbf{x}_{f0}^T\} = 0, \quad (15)$$

and the covariance matrix are defined by

$$\begin{aligned} {}^fP_f &= E\{{}^f\mathbf{v}_f {}^f\mathbf{v}_f^T\}, \quad {}^oP_f = E\{{}^o\mathbf{v}_f {}^o\mathbf{v}_f^T\} \quad \text{and} \\ {}^vP_o &= E\{{}^v\mathbf{v}_o {}^v\mathbf{v}_o^T\}. \end{aligned} \quad (16)$$

Here fP_f is the covariance matrix which describes the uncertainty of the feature in the feature coordinate system, oP_f is the matrix which describes the uncertainty of the feature's position, and vP_o is the matrix which describes the uncertainty of the object in the vehicle coordinate system. With the assumption that no correlations between the values occur, the expectation values of the uncertainty description is given with

$$\begin{aligned} {}^vP_f &= E\{{}^v\mathbf{x}_f {}^v\mathbf{x}_f^T\} \\ &= {}^vP_o + C_{o \rightarrow v} ({}^oP_f + C_{f \rightarrow o} {}^fP_f C_{f \rightarrow o}^T) C_{o \rightarrow v}^T \end{aligned} \quad (17)$$

The last transformation is from the vehicle coordinate system to the measurement coordinate system. This is done using the standard transformation of the discrete state space system and is given with

$${}^m\hat{\mathbf{y}}_f = C_{v \rightarrow m} {}^v\hat{\mathbf{x}}_f \quad (18)$$

$${}^mU_f = C_{v \rightarrow m} {}^vP_f C_{v \rightarrow m}^T + {}^mR \quad (19)$$

where ${}^m\hat{\mathbf{y}}_f$ is the transformed feature in the measurement space, mR is the covariance of the measurements and mU_f is the covariance of the feature in the measurement space. With these equations, the prediction of every feature in the measurement space is given for linear transformations.

In the case of non linear transformations, the estimated mean value of the feature in the vehicle coordinate system is given with

$${}^v\hat{\mathbf{x}}_f = g_{o \rightarrow v}({}^v\mathbf{x}_{o0}, g_{o \rightarrow v}({}^o\mathbf{x}_{f0})). \quad (20)$$

To calculate the expectation value of the uncertainties, the nonlinear transformations has to be linearized by the calculation of the Jacobi matrix, and with this local linearization the covariance matrix is given with

$${}^vP_f = {}^vP_o + \tilde{C}_{o \rightarrow v} ({}^oP_f + \tilde{C}_{f \rightarrow o} {}^fP_f \tilde{C}_{f \rightarrow o}^T) \tilde{C}_{o \rightarrow v}^T, \quad (21)$$

where \tilde{C} denotes, that the linearized C is used. Also in the nonlinear case, the last transformation of the feature in the measurement space is given with

$${}^m\hat{\mathbf{y}}_f = g_{v \rightarrow m}({}^v\hat{\mathbf{x}}_f) \quad (22)$$

$${}^mU_f = \tilde{C}_{v \rightarrow m} {}^vP_f \tilde{C}_{v \rightarrow m}^T + {}^mR. \quad (23)$$

With the feature uncertainty description which is introduced in this section, every feature has its own uncertainty. This is an advantage in those cases where the position of the feature is not exactly known, or the feature itself is applied with uncertainty.

3 Suitable Dynamic Models for Different Object Types

In [3], the dynamic behavior of the objects are modelled with a dynamic model that is based on the assumption of constant acceleration in the two horizontal directions of the vehicle coordinate system. The heading of vehicles was previously defined as the driving direction of the sensor carrying vehicle. This is a reasonable assumption for tracking a vehicle which is in front of the sensor carrying vehicle and is driving in the same direction. In more complex scenes including intersections and oncoming traffic, this assumption is often not true. But the correct inclusion of the heading greatly improves the tracking with the 3D feature model for several object types. Therefore, the usage of a different dynamic model for tracking vehicles is proposed. This *ctrv*-model was already used in other applications to estimate the position and heading of the sensor carrying car [11]. The movement model is based on the bicycle model and assumes a constant yaw-rate and a constant velocity in one observation interval. Besides the position estimate it also allows the estimation of the vehicles' heading. The model limits the possible object's movement according to the limitations of the vehicle's movement.

In addition to the dynamic parameters, the state space contains the object's size, given as width, height and length. This leads to the state space

$$\mathbf{x}_o(t_k) = \begin{bmatrix} v_{x_o}(t_k) \\ v_{y_o}(t_k) \\ v_{\gamma_o}(t_k) \\ v_{v_o}(t_k) \\ v_{\dot{\gamma}_o}(t_k) \\ {}^o w_o(t_k) \\ {}^o h_o(t_k) \\ {}^o l_o(t_k) \end{bmatrix} = \begin{bmatrix} x\text{-position} \\ y\text{-position} \\ \text{heading} \\ \text{velocity} \\ \text{yaw rate} \\ \text{object' s width} \\ \text{object' s height} \\ \text{object' s length} \end{bmatrix}, \quad (24)$$

where the estimated position is the position of the centered rear end of the vehicle and the velocity is the velocity in the driving direction. The state transition equation of the first five elements of the state space is related to the movement description of the nonlinear movement model, while the parameters of the objects size do not change dynamically between two time steps. This leads to the functional description of the nonlinear state transition between t_k and t_{k+1} :

$$\mathbf{x}_o(t_{k+1}) = g_a(\mathbf{x}_o(t_k), T) = \begin{bmatrix} v_{x_o}(t_k) + \cos(v_{\gamma_o}(t_k))a - \sin(v_{\gamma_o}(t_k))b \\ v_{y_o}(t_k) + \sin(v_{\gamma_o}(t_k))a + \cos(v_{\gamma_o}(t_k))b \\ v_{\gamma_o}(t_k) + v_{\dot{\gamma}_o}(t_k)T \\ v_{v_o}(t_k) \\ v_{\dot{\gamma}_o}(t_k) \\ {}^o w_o(t_k) \\ {}^o h_o(t_k) \\ {}^o l_o(t_k) \end{bmatrix} \quad (25)$$

with

$$a = \frac{v_{v_o}(t_k) \sin(v_{\dot{\gamma}_o}(t_k)T)}{v_{\dot{\gamma}_o}(t_k)} \quad (26)$$

$$b = \frac{v_{v_o}(t_k)(1 - \cos(v_{\dot{\gamma}_o}(t_k)T))}{v_{\dot{\gamma}_o}(t_k)}. \quad (27)$$

where T is the time difference between t_k and t_{k+1} . In the special case of a straight forward movement of the vehicle, the function $g_a(\mathbf{x}_o(t_k), T)$ is reduced to

$$g_a(\mathbf{x}_o(t_k), T) = \begin{bmatrix} v_{x_o}(t_k) + \cos(v_{\gamma_o}(t_k))v_{v_o}(t_k)T \\ v_{y_o}(t_k) + \sin(v_{\gamma_o}(t_k))v_{v_o}(t_k)T \\ v_{\gamma_o}(t_k) \\ v_{v_o}(t_k) \\ v_{\dot{\gamma}_o}(t_k) \\ {}^o w_o(t_k) \\ {}^o h_o(t_k) \\ {}^o l_o(t_k) \end{bmatrix}. \quad (28)$$

The described dynamic model is used for tracking cars, bicycles and trucks. For tracking pedestrians the model of constant acceleration is used, because this model seems to be suitable for pedestrians in most situations with respect to the way they move.

An additional function is included to compensate the influence of the movement of the sensor carrying vehicle (refer to [1]). It is based on the measurement of the velocity $v_s(t_k)$ and of the yaw-rate $\dot{\gamma}_s(t_k)$ of this vehicle which is used as an input vector

$$\mathbf{u}(t_k) = \begin{bmatrix} v_s(t_k) \\ \dot{\gamma}_s(t_k) \end{bmatrix}, \quad (29)$$

where the index s denotes the sensor carrying car. With this input vector, the observation of the additional objects displacement due to the sensor carrying vehicle movement is realized on the basis of the constant circle movement model (see figure 5). The velocity and yaw rate are used to com-

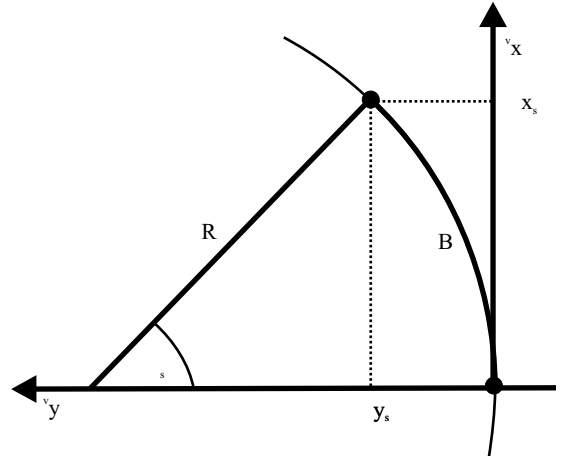


Fig. 5: Constant circle movement model

pute the arc length B and the Radius R

$$B = v_s(t_k) T, \quad R = \frac{v_s(t_k)}{\dot{\gamma}_s(t_k)}. \quad (30)$$

With B and R , the change of the vehicle coordinate system between two times is given by

$$\Delta\gamma_s(t_k) = \frac{B}{R} \quad (31)$$

$$\Delta x_s(t_k) = R \sin(\Delta\gamma_s(t_k)) \quad (32)$$

$$\Delta y_s(t_k) = R(1 - \cos(\Delta\gamma_s(t_k))). \quad (33)$$

The last step is the transformation of the change of the vehicle coordinate system into the corresponding object displacement of the observed objects. This is done by the transformation

$$\begin{bmatrix} \Delta x_o(t_k) \\ \Delta y_o(t_k) \end{bmatrix} = A^{-1} \begin{bmatrix} v x_o(t_k) - \Delta x_s(t_k) \\ v x_o(t_k) - \Delta y_s(t_k) \end{bmatrix} - \begin{bmatrix} v x_o(t_k) \\ v y_o(t_k) \end{bmatrix} \quad (34)$$

$$\Delta\gamma_o(t_k) = -\Delta\gamma_s(t_k) \quad (35)$$

with the rotation matrix

$$A = \begin{bmatrix} \cos(\Delta\gamma_s(t_k)) & -\sin(\Delta\gamma_s(t_k)) \\ \sin(\Delta\gamma_s(t_k)) & \cos(\Delta\gamma_s(t_k)) \end{bmatrix}. \quad (36)$$

To include this displacement, this nonlinear function $g_b(\mathbf{u}(t_k))$ which is given by equation (34) is added to the prediction equation of the Kalman filter.

4 Pedestrian and Vehicle Feature Model

The definition of features is not only dependent on the measurement principle of the sensors, but also on the type of the tracked object. In this section, two different object types are considered and a selection of features are given for two sensors, namely the IR-camera and the laser scanner. The object types under consideration are the most common types in the traffic environment: pedestrians and vehicles. As already mentioned in the above section, the two types are applied with different movement models which influence the selected features.

First, the vehicle object type is described. The movement model of this type is the *ctrv*-model and the state space contains (beside other values) the heading, width, length and height of the object. The basic model is a 3D box which is also defined by its position and heading (see figure 6). The laser scanner features are based on the fact that the laser scans a horizontal plane which is parallel to the ground. In this plane, the vehicle appears as a headed rectangle. The features are defined as cutting points between the rectangle and the laser spots of the laser scanner. This is described in more detail in the next section.

In the IR-camera image, heated surfaces are brighter than the environment. This is used in the pre-processing part which delivers the position and size of all the heated parts, found in the image. On a vehicle, the following parts normally cause heated spots in the IR-image: wheels, exhaust, lights and the radiator. The positions of the features and the transformations are described in more detail in [3].

One of the main differences between the two object types is that the movement model which is used for the pedestrians gives no reliable indication about the heading of the pedestrian. Therefore, the state space includes just width

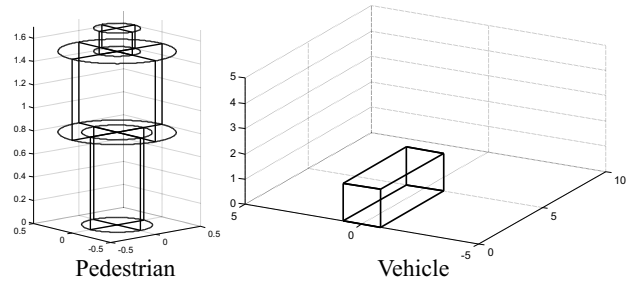


Fig. 6: 3D pedestrian and vehicle description

and height. The basic idea for the description of pedestrians is the usage of several cylinders (see figure 6), because this is a suitable object description, considering the used dynamic movement model.

The cutting plane between the laser plane and the 3D object is a circle, including the assumption that the object is vertically orientated and the laser plane is horizontally orientated. Therefore, the predicted range of a single laser spot r_i results from the cutting point of a straight line with a circle. Basically, the calculation is done similarly to the calculation of the feature for vehicles which is presented in the next section.

In the IR image, the heated spots of pedestrians can normally be divided into three parts: The head, the body and the legs. These are the three cylinders shown in figure 6. Additionally, the legs could be divided into two features, one for each leg. The arms can also be seen as separate features.

5 The Feature Description of Vehicles in the Laser Scanner

As mentioned in the previous section, a special way of using features with a laser scanner is proposed in this section. This method demonstrates the great benefit in combination with orientated objects and with the dynamic *ctrv* model which was described in section 3. Therefore, the example of tracking a vehicle is used as an explanation. If a vehicle enters the horizontal scanning plane of the laser scanner, several single laser spots are reflected and the laser measures a certain distance under these angles. This is illustrated in figure 7.

Some approaches use segmentation algorithms, in order to combine all measurements which belong to one physical object (e.g. [12], [13]). This causes problems when objects are located near to each other and are overlapping partly. In this approach, every cutting point between a laser spot and the predicted vehicle generates a feature. This is possible because the angular resolution and the angles of the laser spots are known. The transformation is nonlinear as given in equation (37), where additionally the transformation also depends on the laser spot angle α_i :

$${}^v \hat{\mathbf{x}}_i = g_{o \rightarrow v}({}^v \mathbf{x}_{o0}, \alpha_i, g_{o \rightarrow v}({}^o \mathbf{x}_{f0})). \quad (37)$$

The transformation into the measurement space (see equation 22) is also nonlinear and the prediction of the i -th fea-

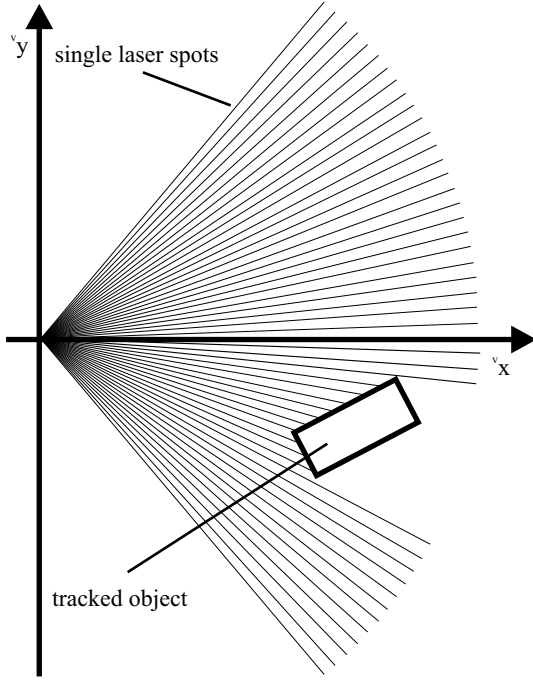


Fig. 7: Vehicle object in the laser plane

ture is the radius r_i :

$$l_{y^*}_i = r_i. \quad (38)$$

This nonlinear function is derived in the following part of the section.

Knowing the laser spot angle α_i and the obstacle's heading, the calculation of the predicted range r_i can be done using the equation for the crossing point of two straight lines

$$x_s = \frac{b_2 - b_1}{m_1 - m_2}, \quad (39)$$

where b is the offset and m the slope of the straight line. The index 1 denotes the parameters of the laser spot. b_1 is zero and the slope is given with $m_1 = -\cot(\alpha)$. The offset

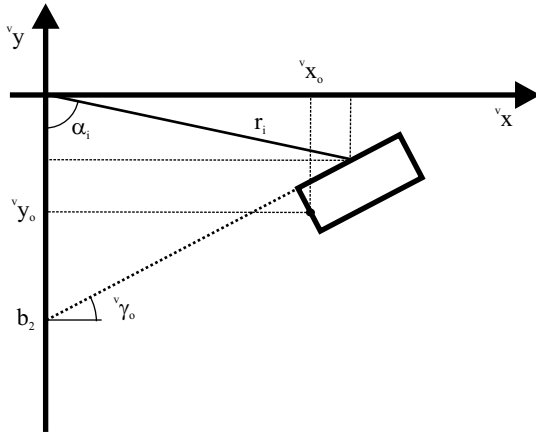


Fig. 8: Geometric relations for the calculation of b_2

of the straight line, which belongs to the vehicle (for the example the left side of the vehicle is used, see figure 8),

can be calculated from the predicted state, using geometric relations

$$b_2 = v_{y_o}(t_k) + \frac{1}{2} v_{w_o}(t_k) \cos(v\gamma_o(t_k)) - \tan(v\gamma_o(t_k)) \left(v_{x_o}(t_k) - \frac{1}{2} v_{w_o}(t_k) \sin(v\gamma_o(t_k)) \right) \quad (40)$$

With x_s and the angle of the laser spot, the predicted feature range for the i th laser spot and the left side of the vehicle is given with

$$r_i = \frac{b_2}{\sin(\alpha_i) (-\cot(\alpha_i) - \tan(v\gamma_o(t_k)))} \quad (41)$$

From (40) and (41), with simplification, r_i is given as

$$r_i = \frac{-\cos(v\gamma_o(t_k)) v_{y_o}(t_k)}{\cos(v\gamma_o(t_k) - \alpha_i)} - \frac{\frac{1}{2} v_{w_o}(t_k) + v_{x_o}(t_k) \sin(v\gamma_o(t_k))}{\cos(v\gamma_o(t_k) - \alpha_i)}. \quad (42)$$

This calculation is done for all cutting points between the predicted vehicle and the laser spots.

6 Initialization of Filters

The initialization of the objects is one of the key functions of multi sensor tracking systems [14]. Usually, new tracks are generated using the following algorithm: if one of the used sensors delivers a new detection which can not be assigned to an existing object (filter) it is labelled as an unknown detection. With this detection, a new filter is set up, but the filter is not confirmed at this time. If more measurements occur in this region during the next fusion steps, the filter is labelled as a confirmed object. In the case of using the generalized feature model, the initialization becomes more difficult. This is for two reasons:

- A transformation is necessary to create a new track on the basis of a new detection. This transformation becomes difficult if no additional information about the detection (e.g. to which feature the detection should be assigned) is available.
- When the first unknown detection of a new object is delivered by the sensors, the class of the new object is unknown. So the initialization algorithm is not able to define which of the feature models (e.g. vehicle or pedestrian model) has to be used.

To overcome these difficulties, a special type of multiple model filter is proposed. This MMF generates a list of filter hypotheses for every detection. Every hypothesis sets up a new filter under the assumption that the detection can be linked to one single feature of a new object. Additionally, filter hypotheses are set up for every possible object class using the different feature models (therefore it is called a multiple model filter). For every fusion step the distances between predicted features and detections are calculated, to define how well the detections fit the hypothesis. After a few fusion steps, unlike hypothesis (hypothesis, where the distances between predicted features and detections is large) are removed. At the end, the most fitting filter hypothesis is labelled as the confirmed object.

7 Results and Conclusions

To verify the functionality of the feature model and to compare the model to other approaches, simulations have been done. For these simulations, the movement of a vehicle was modelled on the basis of the bicycle model. In order to simplify, the sensor carrying vehicle is not moving during the simulation. One of the simulation tracks is shown

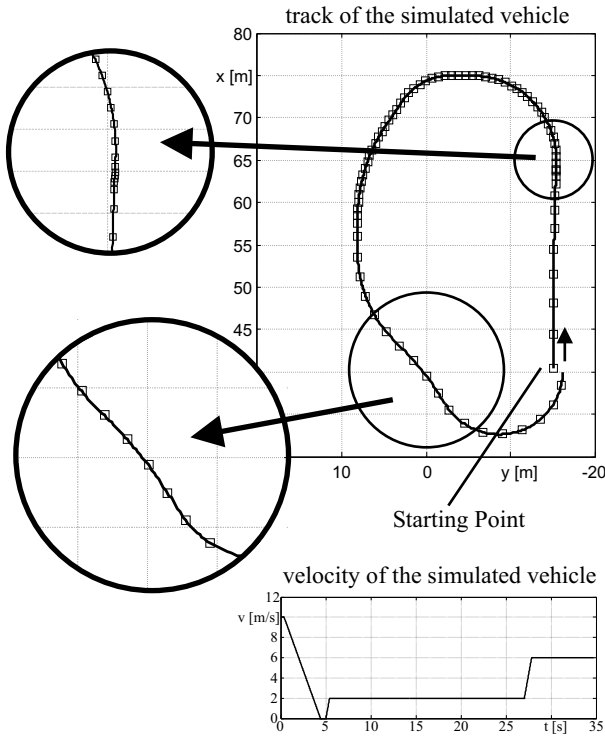


Fig. 9: Simulated track

in figure 9. Different curves and also different velocities are included in the course. On the basis of this track, the measurements of different sensors has been calculated. A reasonable disturbance is added for every sensor and then the data is stored as sensor measurements.

In the following part of the section, the results of two simulations are shown and described. The first simulation is performed only with the laser scanner. The processing of the laser data is done in two different ways, while the dynamic model is the same as described in section 3. The first is the feature approach, which was presented in the previous section. The second is a standard approach where all laser beams which hide the same obstacle are combined and an average of the angles and the shortest range are calculated and used as measurement. Both these approaches are compared and the results are given below. In figure 10 and 11 the errors of the estimated x and y -positions are shown for both models. It is visible that the feature model gives the much better results in comparison to the standard model. The reason is that the standard model includes the assumption that the nearest measured range gives the position of the rear end of the tracked vehicle. And also the assumption that the average of all angles is the middle point of the rear end of the vehicle. Nevertheless, when the presented

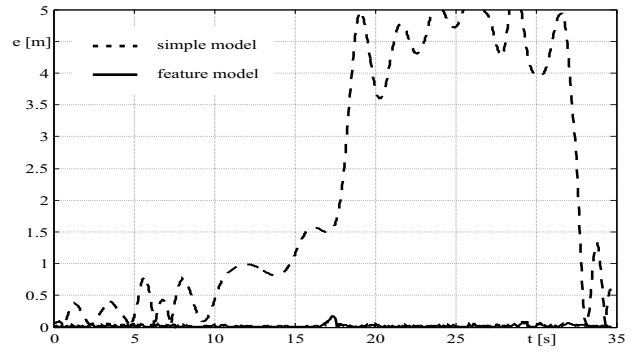


Fig. 10: Comparisons between feature and standard model, x -position

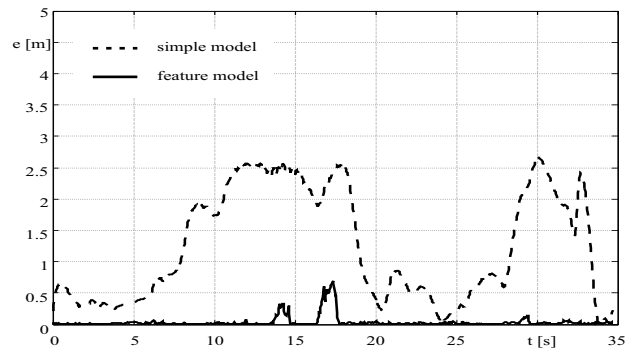


Fig. 11: Comparisons between feature and standard model, y -position

feature model of the laser scanner is used, good results of the position estimates are achieved. Another benefit of the

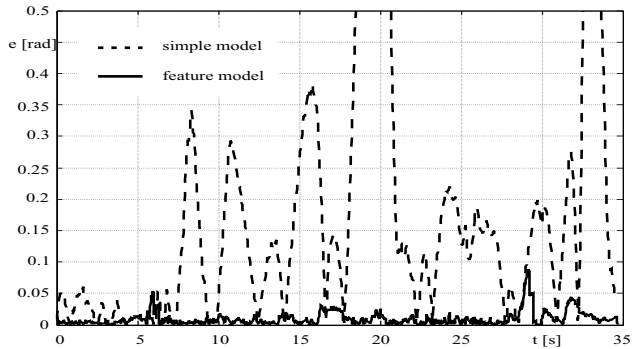


Fig. 12: Comparisons between feature and standard model, orientation angle

feature model is that the heading of the tracked object can be estimated with higher accuracy. The standard model is just able to estimate the heading from the position measurement over time, while the feature model also estimates the heading directly from the measured data. This is shown in figure 12.

The second simulation shows the case of multi sensor multi target tracking. The second sensor is an IR-camera, which shows the heated spots according to the hot surface regions of the vehicle. Most of the time, the results are com-

parable to the case of the single sensor tracking. However, when the tracked target is far away, and the heading of the car is such that only the side of the vehicle is visible for the laser sensor, the second sensor reduces the position estimation error significantly. This happens between simulation time 16 and 18 and can be seen in figure 13.

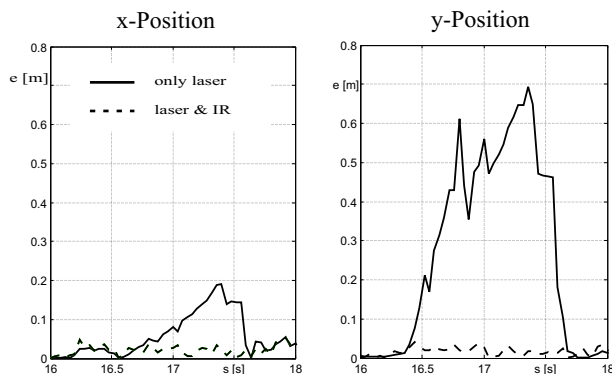


Fig. 13: Single and multi sensor feature model

The first results with real data, collected with an electromobil car on big parking areas as well as in traffic situations, show comparable results.

Summarizing the paper, the usage of a general 3D feature model has been presented, which allows the use of different sensor types integrated in one multi sensor detection and tracking system. Different 3D objects can be modelled adequately by using features distributed in the 3D object space. As shown in simulations, the approach reduces the errors of position and heading estimation significantly. This increases the overall system performance of those multi sensor tracking systems.

References

- [1] U. Scheunert, H. Cramer, A. Polychronopoulos, A. Amditis, G. Wanielik, and P.-C. Antonello. Multi sensor data fusion for object detection: challenges and benefit. In *Proc. of ATA-conference ADAS, Siena, Italy*, 2002.
- [2] K. Weiss, D. Stueker, and A. Kirchner. Target modeling and dynamic classification for adaptive sensor data fusion. In *Proceedings of IV 2003, IEEE Intelligent Vehicles Symposium*, 2003.
- [3] H. Cramer, U. Scheunert, and G. Wanielik. Multi sensor fusion for object detection using generalized feature models. In *Proceedings of the Sixth International Conference on Information Fusion, ISIF*, pages 2–10, 2003.
- [4] E. D. Dickmanns. *4D-Szenenanalyse mit integralen raumzeitlichen Modellen*, volume 149 of *Informatik Fachberichte, Mustererkennung 1987*. Springer Verlag, 1987.
- [5] K. Rohr and H.-H. Nagel. *Modellgestuetzte Bestimmung des Bewegungszustandes von Fussgaengern in Realbildfolgen*, volume 254 of *Informatik Fachberichte, Mustererkennung 1990*. Springer Verlag, 1990.
- [6] A. Amditis, A. Polychronopoulos, I. Karaseitanidis, G. Katsoulis, and E. Bekiaris. Multiple-sensor-collision avoidance
- [7] R. Niu, P. Varshney, K. Mehrotra, and C. Mohan. Temporal fusion in multi-sensor target tracking systems. In *Proceedings of the Fifth International Conference on Information Fusion, ISIF*, pages 812–817, 2002.
- [8] E. Waltz. *The Principle and Practice of Image and Spatial Data Fusion*, volume 4 of *Handbook of Multisensor Data Fusion*, D. Hall, J. Llinas. CRC Press LLC, 2001.
- [9] Y. Bar-Shalom and X. Li. *Estimation and Tracking: Principles, Techniques and Software*. Artech House, Delharn, 1993.
- [10] K. Brammer and G. Siffing. *Kalman Bucy Filter: Deterministische Beobachtung und stochastische Filterung*. R. Oldenburg Verlag, Muenchen, Wien, 1994.
- [11] U. Scheunert, H. Cramer, and G. Wanielik. Multi-sensordaten-fusion in strassenumgebungen. In *Proc. DGON Symposium: Positionierung und Navigation, Dresden (Germany)*, 2003.
- [12] S. Santos, J. Faria, F. Soares, R. Araujo, and U. Nunes. Tracking of multi-obstacles with laser range data for autonomous vehicles. In *Proceedings of ROBOTICA - 3 Festival Nacional de Robotica, Lisboa*, 2003.
- [13] K. Dietmayer, J. Sparbert, and D. Streller. Model based object classification and object tracking in traffic scenes. In *Proceedings of IV 2001, IEEE Intelligent Vehicles Symposium*, pages 25–30, 2001.
- [14] Y. Bar-Shalom and X. Li. *Multitarget-Multisensor Tracking: Principles and Techniques*. YBS Publishing, Storrs, 1995.

system for automotive applications using an imm approach for obstacle detection. In *Proceedings of the Fifth International Conference on Information Fusion, ISIF*, pages 812–817, 2002.